

Article ID: 1006-8775(2016) 03-0352-10

A STUDY ON THE MECHANISM OF RAPID WEAKENING OF TYPHOON XANGSANE (0020) OVER THE EAST CHINA SEA

QIAN Yan-zhen (钱燕珍)¹, ZHANG Sheng-jun (张胜军)², CHEN Lian-shou (陈联寿)²

(1. Ningbo Meteorological Observatory, Hangzhou 315012 China; 2. State Key Laboratory of Severe Weather, Chinese Academy of Meteorological Sciences, Beijing 100081 China)

Abstract: Using the National Center for Environmental Prediction reanalysis data on $1.0^{\circ} \times 1.0^{\circ}$ grids and data from the Tropical Cyclone yearbook (2000), a diagnostic analysis and numerical simulation were performed to investigate the characteristics and mechanism underlying the rapid weakening of typhoon Xangsane. The results show that a sharp decline in the intensity of typhoon Xangsane resulted from its movement into the cool sea surface temperature area in the East China Sea, the intrusion of cold air from the mainland into the typhoon, and a rapid increase of the vertical wind shear in the surrounding environment. An important factor that led to the demise of the typhoon was a significant decrease in the moisture transport into the typhoon. Furthermore, the results of the numerical simulation and sensitivity experiments indicate that sea surface temperature largely modulated the rapid weakening of typhoon Xangsane.

Key words: Typhoon Xangsane; rapid weakening; diagnostic analysis; numerical simulation; structural analysis

CLC number: P444 **Document code:** A

doi: 10.16555/j.1006-8775.2016.03.009

1 INTRODUCTION

The western North Pacific is the basin with the most tropical cyclone (TC) geneses worldwide (Chen and Ding^[1]). China is one of the countries that are in a high risk of severe impacts by TCs. TC impact is directly linked to the TC structure and intensity. Yan proposed a criterion to identify the rapid intensification of TCs, i.e., the absolute value of the maximum wind speed change near a TC center must be greater than or equal to $10 \text{ m} \cdot \text{s}^{-1}$ within 12 h^[2]. Using this criterion, he analyzed the distribution characteristics of rapid changes in the TC intensity over the western North Pacific. Yu et al. utilized the minimum sea-level pressure at a TC center to measure the TC intensity and established a standard to denote the sudden intensification of TCs^[3]. Duan et al. summarized previous research on TC intensity changes, including TC genesis and extreme TC intensity, as well as the environmental effects on TC intensity changes^[4]. Yu and Zeng et al. investigated the characteristics and mechanism of the offshore rapid intensification of super-typhoon Saomai (2006) through

analysis and numerical simulation^[5,6]. These studies primarily focused on the intensification or rapid intensification of TCs. However, most TCs tend to weaken because of changes in their underlying surfaces when approaching land. In these cases, it is usually not difficult to forecast the slow intensity changes of offshore TCs. Nevertheless, the rapid weakening of TCs sometimes occurs, e.g., typhoons entering the South China Sea or East China Sea from October onward may undergo rapid weakening and disappear. For such TCs, forecasts may be wrong, and hence, losses may occur owing to the use of excessive preventive measures (Xu et al.^[7], Chen et al.^[8]). On average, since 1949, three or four TCs enter the East China Sea ($23^{\circ} 00' \text{N} - 33^{\circ} 10' \text{N}$, $117^{\circ} 11' \text{E} - 131^{\circ} 00' \text{E}$) every year. However, it is very rare for a TC to rapidly weaken and come to an end after entering the East China Sea. One such case is that of typhoon Xangsane (0020), which formed on October 26, 2000, moved north to northeast after entering the East China Sea, rapidly weakened over that area, and finally decayed. Therefore, investigating the physics and mechanism of the rapid weakening and demise of typhoon Xangsane is vital for improving future TC forecasts and avoiding resource wastage resulting from the use of excessive prevention and mitigation measures.

2 DATA, LARGE SCALE SYNOPTIC AND SATELLITE IMAGERY ANALYSES

2.1 Data

Six-hour pressure differences (Δp) from the Tropical Cyclone Yearbook (2000) were used to identify the TC intensity. The data were available four

Received 2014-10-31; **Revised** 2016-05-22; **Accepted** 2016-07-15

Foundation item: National Key Basic Research Program of China (2015CB452804); National Natural Science Foundation of China (41575063, 41275066, 41075037); Ningbo Science and Technology Project (2014C50024)

Biography: ZHANG Sheng-jun, Ph. D., Researcher, primarily undertaking research on numerical simulation and tropical cyclones.

Corresponding author: ZHANG Sheng-jun, e-mail: zhangsj@camsma.cn

times at a daily basis at 0000, 0600, 1200, and 1800 UTC. The method used in the present study to define rapid changes of the TC intensity was originally proposed by Yu et al.^[3], who defined the rapid weakening of a TC as a phenomenon that occurs when the six-hour increase of the minimum sea-level pressure near the TC center is greater than 8.30 hPa. The data on the intensity of typhoon Xangsane obtained from the USA Joint Typhoon Warning Center (JTWC) and the Regional Specialized Meteorological Center (RSMC) of the Tokyo Typhoon Center were also included in the analysis (Table 1). On November 1, 2000, from 0000 to 0600 UTC, the minimum sea-level pressure at the

typhoon center increased by 20 hPa and the maximum wind speed near the center decreased by approximately $15 \text{ m} \cdot \text{s}^{-1}$. The JTWC data revealed a 13-hPa increase in the minimum sea-level pressure and a $7 \text{ m} \cdot \text{s}^{-1}$ wind decrease near the center. The data from the RSMC Tokyo Typhoon Center revealed a 10-hPa increase in the minimum sea-level pressure and a $6 \text{ m} \cdot \text{s}^{-1}$ decrease in the maximum wind speed near the center. This period showed continuous weakening in all three data sources and satisfied the criterion for rapid weakening. Therefore, in this study, we focused on the rapid weakening of typhoon Xangsane from 1200 UTC on October 31, 2000.

Table 1. Intensity of typhoon Xangsane during its late stages, as indicated by the minimum sea-level pressure at the typhoon center (Units: hPa).

	12 h Oct. 31	18 h Oct. 31	00 h Nov. 1	06 h Nov. 1	12 h Nov. 1	18 h Nov. 1
CMA	965	970	975	995	995	1000
JTWC	963	966	970	983	991	994
JMA	960	965	975	985	992	1000

The present analysis was based on the National Centers for Environmental Prediction (NCEP) reanalysis data, which were obtained four times at a daily basis with horizontal grids of $1^\circ \times 1^\circ$ and 26 vertical levels, as well as on the sea surface temperature (SST)/land skin temperature (LST) data from the Physical Sciences Division (PSD) Climate Data Repository, which were obtained four times at a daily basis with grids of $1.875^\circ \times 1.875^\circ$. Through diagnostic analyses of relevant physical variables, the characteristics and physical mechanisms of the rapid weakening of typhoon Xangsane over the East China Sea were elucidated. The mechanisms were further investigated by numerical simulation and sensitivity experiments using the Advanced Research Weather Research and Forecast model version 3.3 (WRFV3.3).

2.2 Large scale circulations

Typhoon Xangsane (0020) formed southeast of Luzon Island over the western North Pacific at 0600 UTC on October 26. After its formation, it continued moving west to northwest. Starting at 1800 UTC on October 29, after crossing Luzon Island, Xangsane turned north to northeast, passed near shore over the east coast of Taiwan Island, weakened, and decayed going over the East China Sea. Xangsane gradually intensified after its formation, became a severe tropical storm at 0600 UTC on October 27, and was further upgraded into a typhoon at 0000 UTC on October 30. At that time, the minimum sea-level pressure at its center was 965 hPa and the maximum wind speed near the center was $40 \text{ m} \cdot \text{s}^{-1}$; this intensity was sustained for more than 30 h. Typhoon Xangsane weakened after 1200 UTC on October 31 and decayed at 1800 UTC on November 1 (see Fig.1).

During the lifetime of Typhoon Xangsane, a

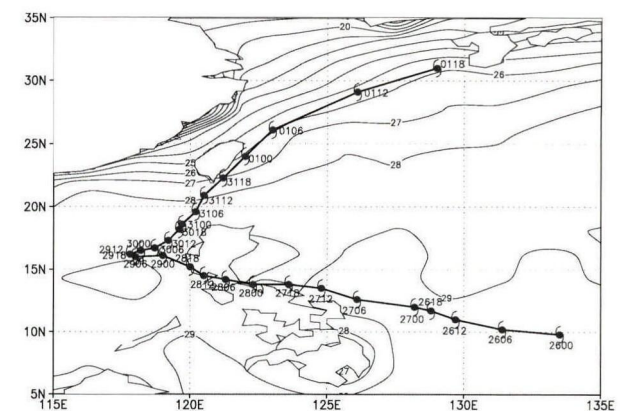


Figure 1. Track of Typhoon Xangsane and SST at 0000 UTC on October 31, 2000.

westerly cold-air trough moved eastward at 500 hPa. At 0000 UTC on October 31 (Fig.2a), the trough was situated at around 105°E – 110°E . It then broke into two branches at 0000 UTC on November 1 (Fig.2b), with the northern branch shifting to 120°E – 125°E and the southern branch remaining at around 110°E but slightly southward. Meanwhile, the subtropical high was quite stable, with the ridge line almost stagnated at around 25°N . Under such a circulation environment, the typhoon during its course of northeastward movement would be affected by the cold air guided by the north branch of the trough only after the typhoon reached or crossed the ridge line.

Obvious cold advection occurred at 850 hPa along the mid-latitude area in the northwest quadrant of Xangsane, and Xangsane was affected by both the southwest monsoon and the southerly at the southwestern side of the subtropical high in the southern

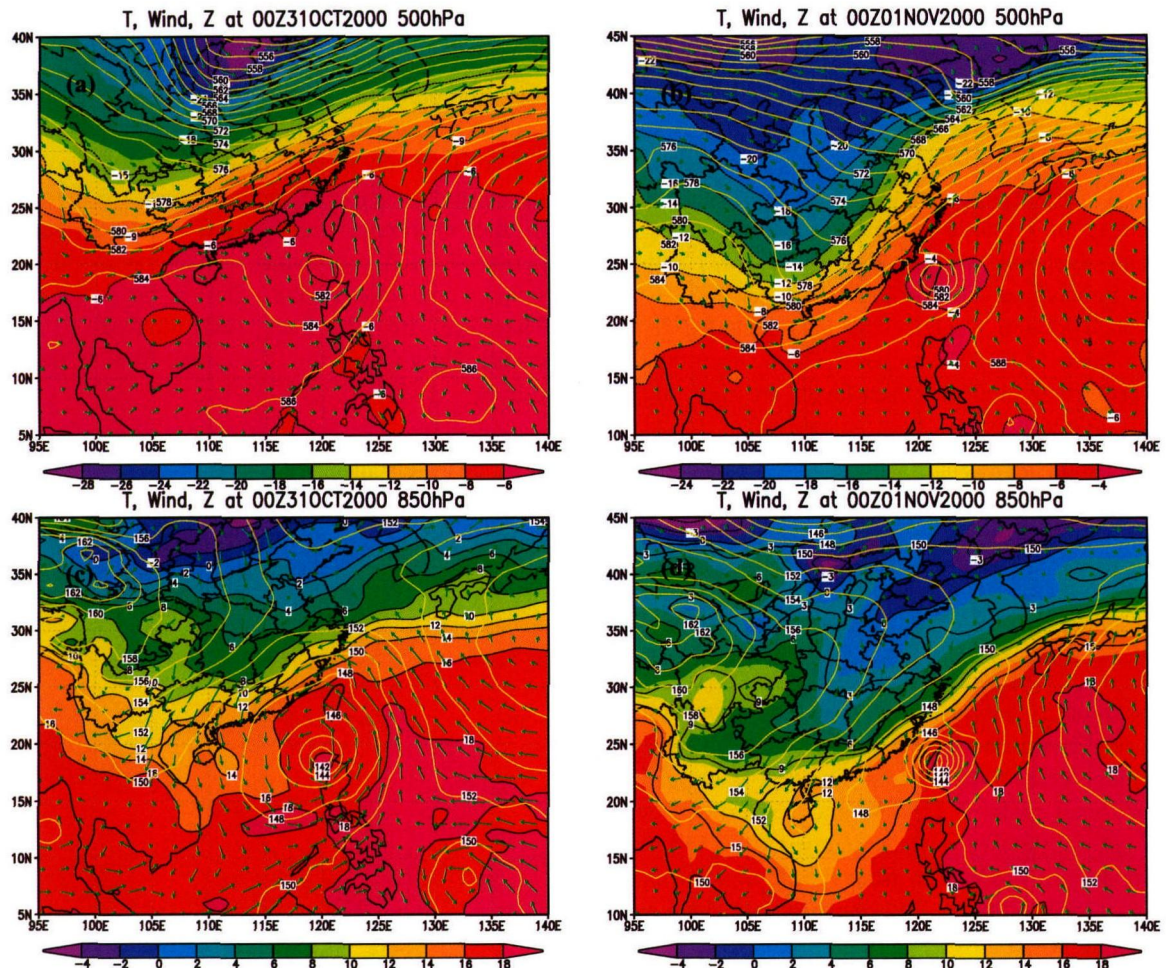


Figure 2. Geopotential height (lines, units: hPa), temperature (shaded, units: $^{\circ}\text{C}$), and wind vector field (units: $\text{m}\cdot\text{s}^{-1}$) at 500 hPa at (a) 0000 UTC on October 31 and (b) 0000 UTC on November 1 and at 850 hPa at (c) 0000 UTC on October 31 and (d) 0000 UTC on November 1 during the weakening phase of Xangsane.

quadrant of Xangsane at 0000 UTC on October 31 (Fig. 2c). At 0000 UTC on November 1, Xangsane had moved to east of Taiwan Island (Fig. 2d). The wind west of Xangsane was weak owing to the presence of Taiwan Island. Meanwhile, cold advection into Xangsane due to the north wind from the west of Xangsane occurred around its northwest outer periphery. South of Xangsane, the southwest monsoon weakened, and Xangsane was mainly affected by the southerly at the western side of the subtropical high.

2.3 Satellite imageries

Satellite images obtained prior to and after the start of the weakening of Xangsane (Fig. 3) revealed that Xangsane did not cover a very large area, with a diameter of less than 500 km. However, the typhoon was well developed, with a well-organized cloud pattern, clear and compact eye, symmetric structure, and brightness temperature at the top of the cloud of less than -70°C , indicating a strong intensity. After 0000 UTC on October 31, as a result of a gradual merging with the cloud system of the westerly trough to the north, the typhoon structure gradually decomposed with

a relatively smaller confined cloud area. However, the brightness temperature did not change much, indicating that the typhoon was still strong. After approaching Taiwan, the typhoon weakened, as demonstrated by a decline in the brightness temperature. As Xangsane moved away from the east coast of Taiwan Island and over the East China Sea, its structure was completely destroyed, and it rapidly weakened in intensity.

3 DIAGNOSTIC ANALYSES ON ENVIRONMENTAL FIELDS AND PHYSICAL VARIABLES

Various physical processes that affect the TC intensity and structure mainly involve dynamic and thermodynamic processes (Chen et al.^[9]). SST and atmospheric thermodynamic structure (e.g., upper-troposphere temperature) are generally considered to be the dominant factors that force TC intensity changes (Emanuel et al.^[10,11]). Large-scale environmental forcing mainly includes vertical wind shear as well as other parameters (Zhang et al.^[12], DeMaria^[13]). Yuan discussed the role of diabatic heating in the genesis and

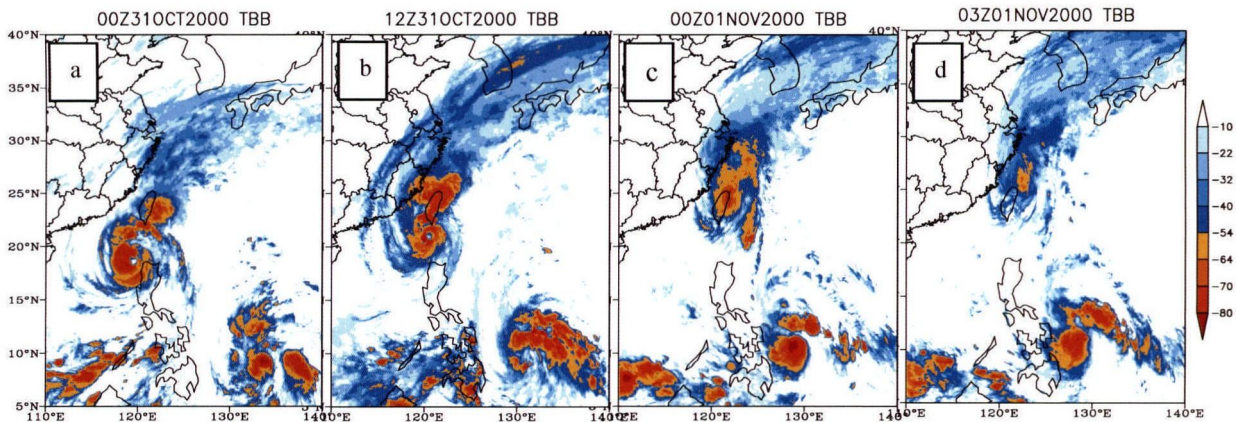


Figure 3. Images of Xangsane prior to and after weakening (units: °C) at (a) 0000 UTC on October 31, (b) 1200 UTC on October 31, (c) 0000 UTC on November 1, and (d) 0300 UTC on November 1.

development of TCs using equations describing moisture and energy budgets^[14]. These previous studies revealed that SST and cold air, etc. were the main factors affecting variations in the TC intensity, and these analyses of moisture supply and vertical wind shear etc. would assist in understanding mechanisms underlying the evolution of TCs.

3.1 Sea surface temperature

SST plays a vital role in TC intensity variation. Observational evidence revealed that TCs can form only over vast oceanic areas with SSTs higher than 26.5°C (Chen and Ding^[1]). Baik et al. reported that 87% of tropical storms in the western North Pacific reached their maximum intensities in life-time when SST was between 27°C and 29°C^[15]. The effects of oceans on the TC intensity arise from various factors such as the ocean heat content, ocean mixing layer depth, and air-sea interactions etc. (Baik et al.^[15], Andreas et al.^[16], Zeng et al.^[17]).

In the present study, SST variations are analyzed with respect to the typhoon’s movement using the SST/LST data from the PSD Climate Data Repository. Fig.1 shows SST at 0000 UTC on October 31 and the track of typhoon Xangsane. It can be observed that SST decreased by approximately 2° during the movement of Xangsane between 1200 UTC on October 31 and 0000 UTC on November 1. Subsequently, Xangsane continued to move toward the colder SST area. Furthermore, based on the relation between mean SSTs in two grids from the typhoon center along each of the four compass directions (east, west, north, and south) and the intensity change of Xangsane (Fig.4), it is apparent that the entry of the typhoon into a low-SST area was a critical factor responsible for its rapid weakening. The correlation between low SST and typhoon weakening can be as high as -0.93. Therefore, the weakening of typhoon Xangsane is well correlated with SST decrease.

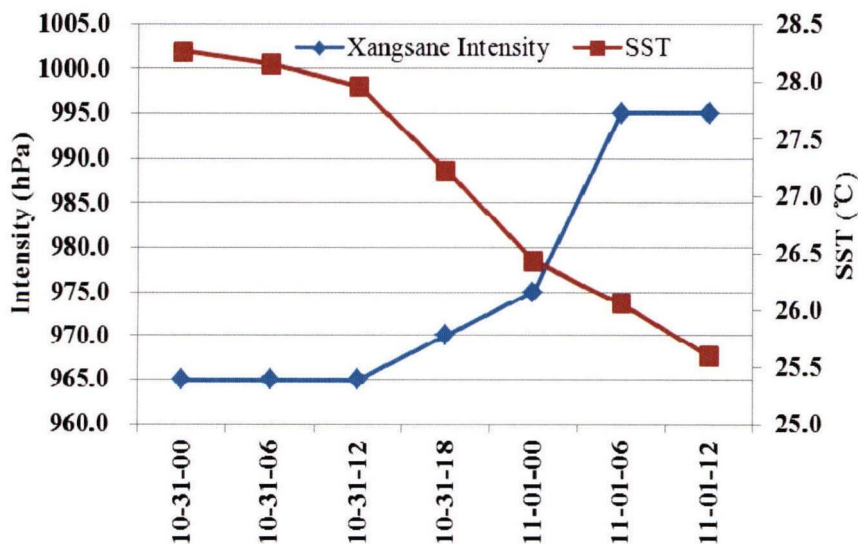


Figure 4. Relation between mean sea surface temperatures associated with movement and intensity changes of typhoon Xangsane (from 0000 UTC on October 31 to 1200 UTC on November 1).

3.2 Vertical wind shear

The major effect of environmental vertical wind shear is to suppress the TC intensity. Yu et al. concluded that vertical wind shear between 200 hPa and 850 hPa favored TC intensification when it was less than $10 \text{ m}\cdot\text{s}^{-1}$ and TC weakening when it was more than $12 \text{ m}\cdot\text{s}^{-1}$ [18]. Fig. 5 displays the variation of vertical wind shear over Xangsane through time. It shows that at a range of five grid lengths from the typhoon center along each direction, the average values of vertical wind shear increased from $13 \text{ m}\cdot\text{s}^{-1}$ to $25 \text{ m}\cdot\text{s}^{-1}$ at 1800 UTC on October 31, constituting favorable conditions for the decline in the typhoon intensity. Wind shear values remained higher than $18 \text{ m}\cdot\text{s}^{-1}$ after 1800 UTC on October 31 and exhibited good correspondence to typhoon weakening with a six-hour time lag.

In this study, we analyze the variations of the U and V components of the wind in the lower level (850 hPa) and upper level (200 hPa) within five grid lengths from the typhoon center along each direction (figures omitted). The results indicate that the difference between the U components of the wind in the lower and higher layers did not significantly change during the rapid weakening of Xangsane. On the other hand, the V component of the wind at the higher layer gradually increased with a maximum range of $4 \text{ m}\cdot\text{s}^{-1}$ at 1800 UTC on October 31, and the difference in the V component between the lower and higher layers reached its maximum at the same time. This suggests that the marked increase in the wind's V component at the higher layer significantly contributed to the rapid weakening of typhoon Xangsane.

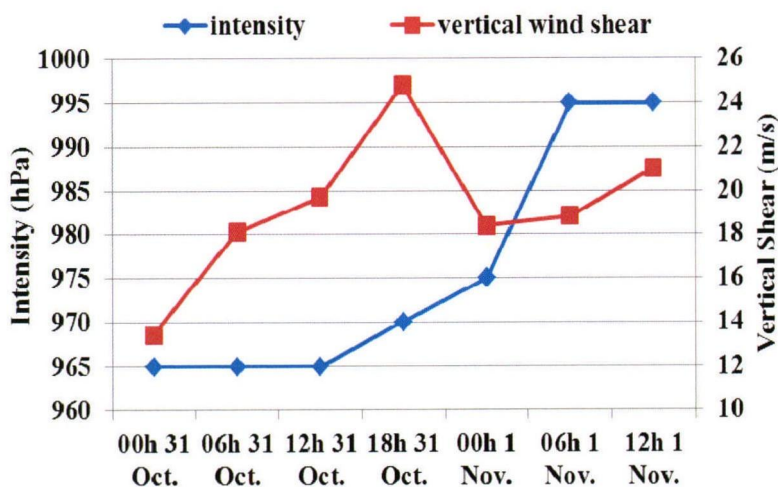


Figure 5. Time variation of vertical wind shear between 200 hPa and 850 hPa and Xangsane intensity (from 0000 UTC on October 31 to 1200 UTC on November 1).

3.3 Cold air

Cold air can either intensify a typhoon or weaken it by destroying its structure (Hanley et al. [19]). To determine the effect of cold air on the typhoon, zonal-vertical cross-sections of temperature and wind vectors are produced along the latitude where the center of typhoon Xangsane was located (Fig.6a, 6b, and 6c). These figures illustrate that updraft movement near the typhoon center appeared above 200 hPa at 0000 UTC on November 1 within a 2° longitude range. Starting at 0600 UTC on November 1, the updraft height was reduced to below 400 hPa, and the updraft area was extended to cover a 4° longitude range. After 12 h, the updraft area near the typhoon faded, became obscure, and markedly deviated from the typhoon center. Comparing Fig.6a, 6b, and 6c, it is evident that the whole atmospheric temperature generally tended to decrease. In the layer from 300 hPa to 500 hPa, cold air moved from west to east and from the upper layer to downward and moved gradually from 111°E to 114°E and subsequently to 117°E in a near-easterly direction.

At 0000 UTC on November 1, a strong downdraft occurred at approximately 2° longitude at the west of the typhoon. This downdraft may have been a factor responsible for the destruction of the warm core of the typhoon. Furthermore, cold air was drawn outside the periphery of the typhoon from west to east in the lower layer below 850 hPa, and the cold air disrupted the warm core structure in the area where the typhoon center was located. Fig. 7a and 7b show zonal-vertical cross-sections of cold advection and horizontal winds along the latitude where the typhoon center was located. Northerly flows west of the typhoon were undermined by mid-upper layer transportation from the southwesterly in front of the trough at 0000 UTC on November 1, and thus, they were significantly affected, although the southwesterly flow in the lower layer was still distant from the typhoon. As a result, the northerly wind west of the typhoon was weaker than the southerly in the east; therefore, the horizontal circulation of the typhoon was destroyed. In fact, cold advection occurred at 0000 UTC on November 1 at approximately 2° of

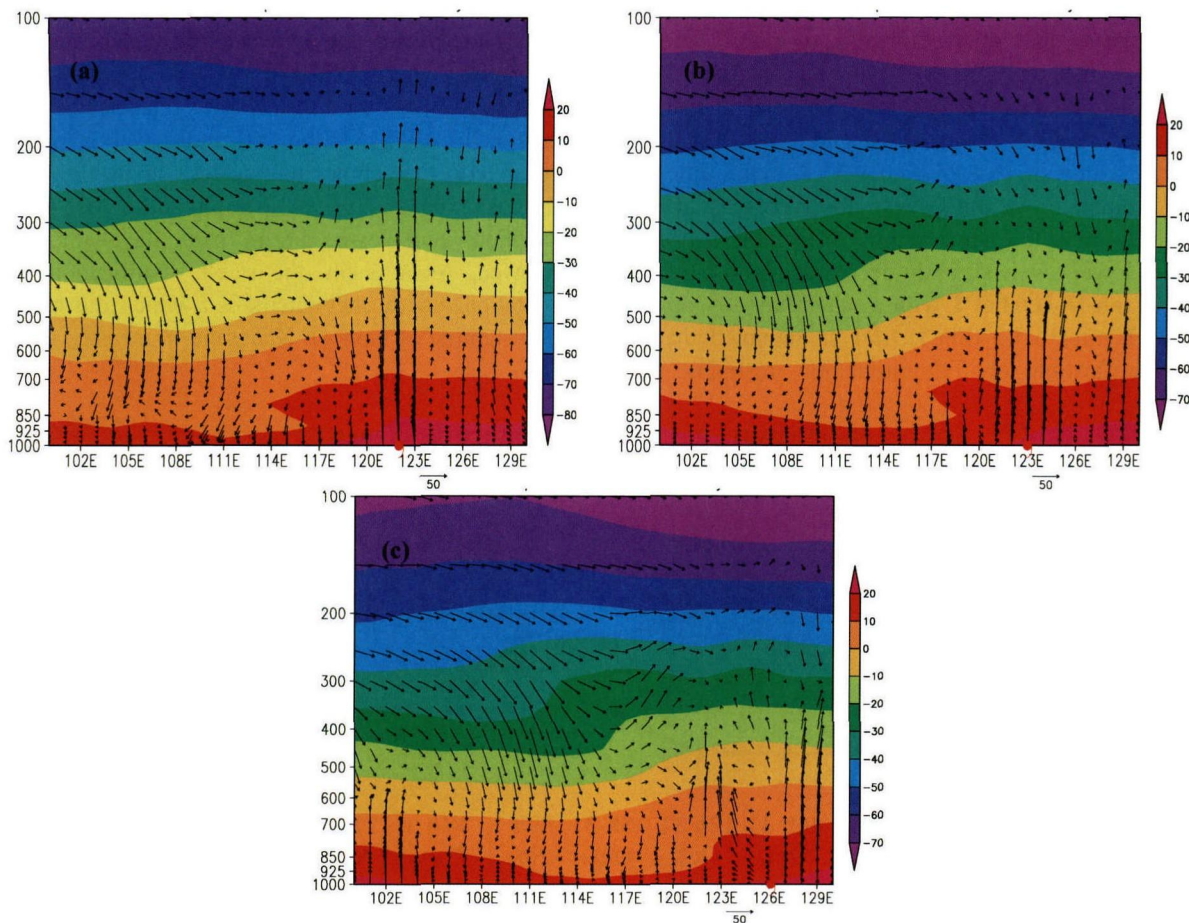


Figure 6. Zonal-vertical cross-sections of temperature (shaded, units: °C) and wind fields at (a) 0000 UTC on November 1, (b) 0600 UTC on November 1, and (c) 1200 UTC on November 1 across the center of typhoon Xangsane.

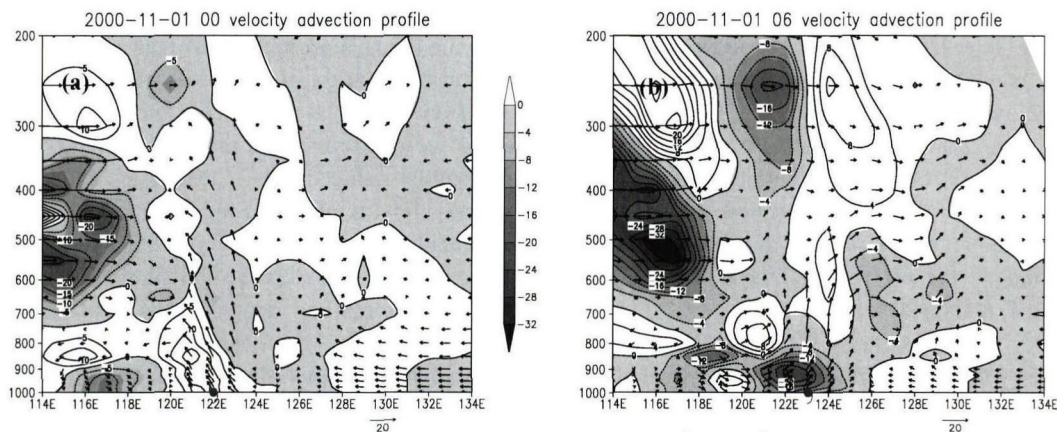


Figure 7. Zonal-vertical cross-sections of cold advection (contour, units: $10^{-3} \cdot m \cdot s^{-1} \cdot ^\circ C \cdot m^{-1}$) and wind fields across the center of typhoon Xangsane at (a) 0000 UTC on November 1 and (b) 0600 UTC on November 1.

longitude away from the typhoon center in the lower level. However, at 0600 UTC on November 1, cold advection had already occupied the lower layer of the typhoon. Such an intrusion by cold advection finally led to the weakening of typhoon Xangsane.

From the evolution of the zonal-vertical cross-sections of the temperature anomaly field across the center of typhoon Xangsane, the effect of cold air

intrusion on the typhoon's temperature structure is revealed. During the period of rapid weakening, the warm core was maintained well within the mid-upper level and the greatest temperature change mainly occurred in the lower level (figures omitted). Before 0000 UTC on November 1, there was a positive temperature anomaly near the center of typhoon Xangsane from the lower to upper layer and the

temperature difference between 850 hPa and 200 hPa remained greater than 65°C. However, at 0600 UTC on November 1, the lower level of typhoon Xangsane was intruded by cold air and an obvious negative temperature anomaly was produced west of the Xangsane center in the lower level. At that time, a positive temperature anomaly was observed only at the upper level, and the temperature difference between upper and lower levels abruptly decreased up to 63°C at 0600 UTC on November 1 with a magnitude of approximately 3°C after 6 h (Fig.8). Lei et al. noted that a stable stratification of TC circulation restrains the

development of a TC [20]. Consequently, a low temperature difference between the upper level (200 hPa) and lower level (850 hPa) is an important factor in TC decay. In this case, we can say that because of the intrusion of cold air from the mid-lower layer of the atmosphere, the temperature pattern in the lower level was destroyed and the temperature difference between the upper and lower layers over the typhoon was narrowed. As a result, the stable stratification of TC circulation was further intensified, which did not favor the sustaining of typhoon Xangsane's intensity.

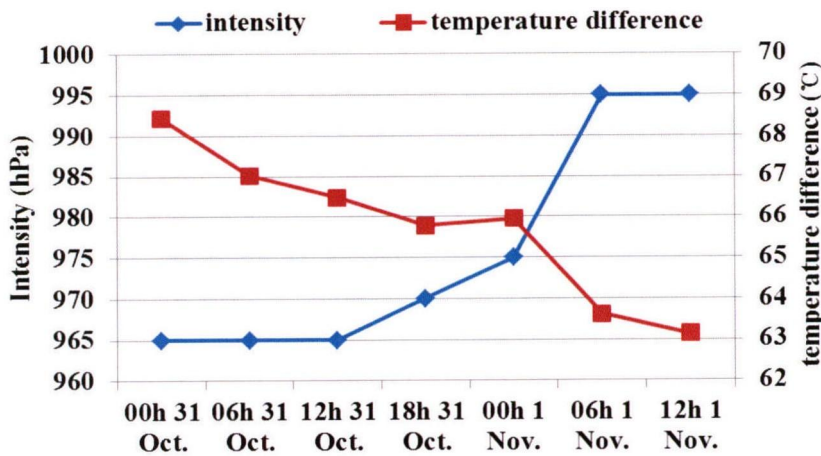


Figure 8. Time variation of temperature difference between 200 hPa and 850 hPa and observed intensity of Xangsane (from 0000 UTC on October 31 to 1200 UTC on November 1).

3.4 Moisture

Moisture supply is an important factor in sustaining and strengthening TCs. Using eight typhoon positions in the time period between 1200 UTC on October 31 and 1800 UTC on November 1, for an extent of five grid lengths horizontally from each typhoon center in each direction, the moisture budget is computed for four cross-sections in each compass direction using the equations given below. The moisture flux is expressed by F_e , F_s , F_w , and F_n for east, south, west, and north, respectively, and F is their total.

$$F_e = -\frac{1}{g} \int_{\varphi_1}^{\varphi_2} \int_{P_s}^{P_0} q u d p d \varphi, \tag{1}$$

$$F_s = \frac{1}{g} \int_{\lambda_1}^{\lambda_2} \int_{P_s}^{P_0} q v d p d \lambda, \tag{2}$$

$$F_w = \frac{1}{g} \int_{\varphi_1}^{\varphi_2} \int_{P_s}^{P_0} q u d p d \varphi, \tag{3}$$

$$F_n = -\frac{1}{g} \int_{\lambda_1}^{\lambda_2} \int_{P_s}^{P_0} q v d p d \lambda, \tag{4}$$

where P_s is the surface pressure, $P_0 = 100$ hPa, λ is the geographic longitude, and φ is the geographic latitude. The total moisture flux can be expressed as:

$$F = F_e + F_s + F_w + F_n \tag{5}$$

Positive values denote the moisture inflow into the typhoon area; negative values indicate the opposite. In Fig.9, the lines represent horizontal moisture fluxes in the four boundaries of the area where the typhoon is located and the total flux. From the total moisture flux budget, we determine that the total moisture influx was significantly reduced after 1200 UTC on October 31. For the interval when the typhoon intensity started to dramatically weaken, between 0000 UTC and 0600 UTC on November 1, the total moisture flux in Fig.9 also shows a marked decrease and subsequently maintains a low level. A comparison of the moisture fluxes of the four directions shows that the moisture source was mainly located in the east, and there was a major inflow of moisture at the start of the analysis period. However, after 1200 UTC on October 31, the moisture influx gradually decreased. The moisture influx began to substantially decrease from 1800 UTC on October 31 and became negative at 0600 UTC on November 1. To the west, the moisture inflow/outflow varied the least with a constant nominal inflow, although there was an obvious decrease but with a small difference between 0000 UTC and 1200 UTC on November 1. In contrast, the moisture flux to the south exhibited the highest variation. The flux in this direction was dominated by the outflow before 0000 UTC on November 1, which

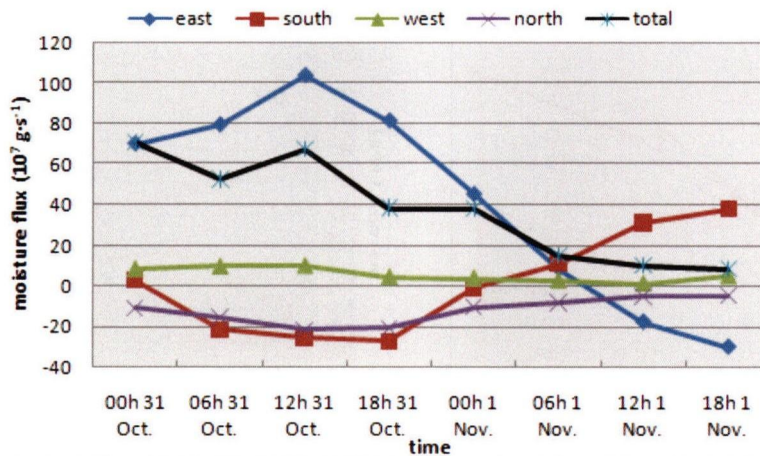


Figure 9. Time variation of water budget (units: $10^7 \cdot g \cdot s^{-1}$) in the column from 1 000 hPa to 100 hPa from 0000 UTC on October 31 to 1800 UTC on November 1.

changed to an inflow after 0006 UTC on November 1. To the north, the moisture outflow always prevailed.

4 NUMERICAL SIMULATION AND ANALYSIS

4.1 Model design

In this study, the new-generation mesoscale numerical model WRFV3.3, which was developed by the National Center for Atmospheric Research, USA, is employed to simulate the weakening of typhoon Xangsane. Two grids are used in the simulation. Grid A has a coarse resolution of 15 km horizontally and 26 Sigma levels in the vertical direction. It is centered at $25.0^\circ N$, $124.0^\circ E$ using double two-way nesting and integrated for 48 h with an initial time of 0000 UTC on October 31, 2000. Grid B has a fine resolution of 5 km, storm-relative centering, and movable nesting. The two grids, A and B, simultaneously start with 60-s and 20-s time steps, respectively. Furthermore, a typhoon bogus is embedded with its center at $18.6^\circ N$, $120.2^\circ E$; $69 m \cdot s^{-1}$ maximum wind speed; 60-km maximum wind radius; and 0.75 maximum wind-speed lapse rate. This experiment is referred to as the control experiment (CNTR for short). The other model specifications are

listed in Table 2. In addition, a sensitivity experiment on SST is performed by increasing SST in the area between $22.86^\circ N$ and $30^\circ N$ to $28^\circ C$ for examining the role of SST in the weakening of typhoon Xangsane (Exp_SST for short).

4.2 Model results

4.2.1 SIMULATION OF TRACK AND INTENSITY

The typhoon track in CNTR is very similar to the best track, except that simulated typhoon movement is slightly slower than that observed (Fig.10a). The track in Exp_SST is very close to that of the control run.

The typhoon intensity simulated by the model basically reflects the observations, particularly for the time during which the typhoon underwent rapid weakening (Fig.10b). From 0000 UTC to 0600 UTC on November 1, 2000, the simulated typhoon intensity in CNTR decreases by 12 hPa, reflecting the rapid weakening of the typhoon during that period. After SST increase, the typhoon weakens by a significantly smaller amount (3.5 hPa) during the same period. The slower rate of weakening is subsequently maintained. The results further verify the role of lower SST during the typhoon weakening stage.

Table 2. Model configuration

Area	Grid A	Grid B
Grid number	260 × 230	301 × 301
Grid size	15 km	5 km
Integration time	0-48 h	0-48 h
Microphysics scheme	WSM6-class graupel scheme	WSM6-class graupel scheme
Cumulus convection parameterization scheme	Kain-Fritsch (new Eta) scheme	no
Land surface process	Noah	Noah
Planetary boundary layer scheme	YSU scheme	YSU scheme
Longwave radiation scheme	RRTM scheme	RRTM scheme
Shortwave radiation scheme	Dudhia scheme	Dudhia scheme

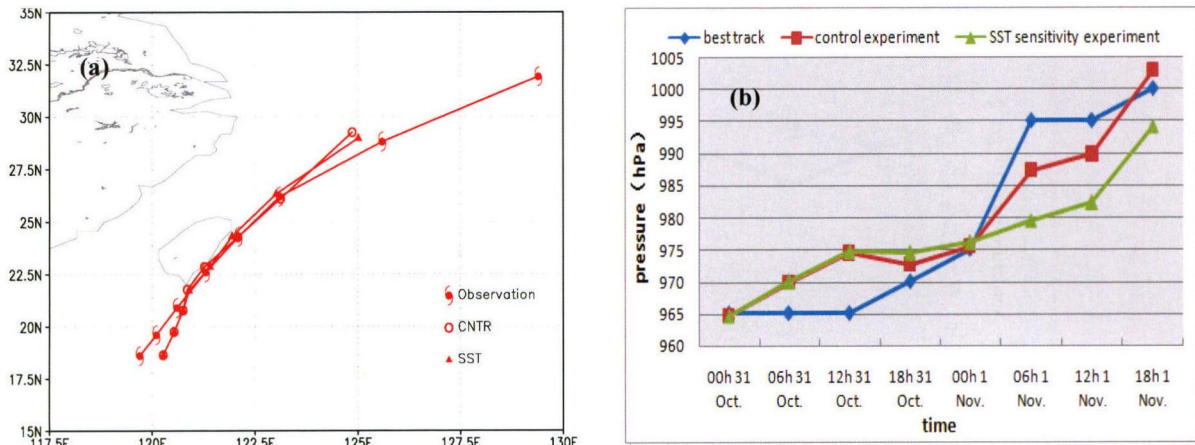


Figure 10. (a) Track and (b) simulated intensity of typhoon Xangsane in CNTR and Exp_SST.

4.2.2 CONTROL EXPERIMENTS

Comparing the simulated maximum radar echo results with satellite images (Fig.2), it appears that the patterns are very similar at 1200 UTC on October 31, before the typhoon started to weaken; at 0000 UTC on November 1, when the typhoon started to undergo rapid weakening; and at 0600 UTC on November 1, when the typhoon had already been weakened (figures omitted). The intensities are fairly similar. Therefore, we generally conclude that the model control experiment well simulates the typhoon and prevailing environmental conditions.

4.2.3 SENSITIVITY EXPERIMENTS

After a change in SST, the air temperature correspondingly changed. An analysis of the simulated temperature difference between the 850-hPa and 200-hPa levels shows that the temperature difference was maintained at around 67°C– 68°C before 0600 UTC on November 1 and appeared to decrease afterward (Fig.11). At 0600 UTC on November 1, the temperature difference began to rapidly decrease, with a maximum magnitude of 2°C – 3°C after 6 h. Compared to the NCEP reanalysis data, the simulated temperature difference in the vertical direction shows a small decrease with a time lag of approximately 6 h.

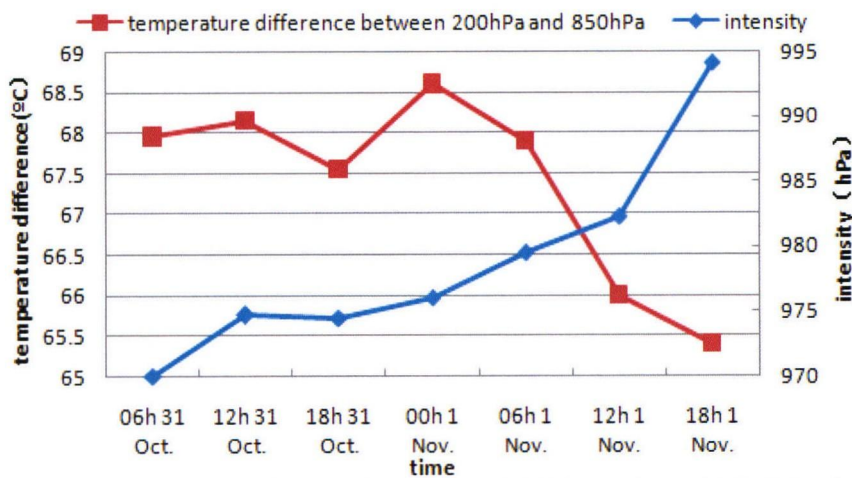


Figure 11. Variation in temperature differences between the 200-hPa and 850-hPa levels with typhoon Xangsane's intensity in Exp_SST.

5 CONCLUDING REMARKS AND DISCUSSION

Based on the diagnostic analysis, the numerical simulation of the late weakening stage, particularly the period of the typhoon's rapid weakening, some initial conclusions may be drawn as follows.

(1) Weakening, in general, and rapid weakening, in particular, of typhoon Xangsane resulted from a

combination of a rapid decrease in SST in the area that the typhoon was entering, an intrusion of cold air from the middle layer downward in the west side of the typhoon, and an intrusion of significant cold advection in the lower layer.

(2) The intensity of the typhoon is closely associated with the moisture supply into the typhoon. A significant reduction in the moisture supply will result in

a rapid weakening of the typhoon. In addition, a strong correlation is obtained between the significant increase in vertical wind shear and the rapid weakening of the typhoon. These correlations will be very useful for the future forecasting of typhoon intensity changes.

(3) The numerical model well simulates the typhoon track and intensity weakening (including the duration of rapid weakening). The simulation results also reflect structural changes in the typhoon. After SST increase, weakening is reduced in intensity and delayed in duration. This result illustrates the role of SST in the weakening of the typhoon. Further analysis and experiments on the effects of SST and cold air on typhoon activity will be performed in a separate study.

Furthermore, we must notice that typhoon Xangsane moved northward along the east side of Taiwan Island, with the typhoon center very close to the island, but not moving across it; this type of typhoon track is rare in history. Although part of typhoon Xangsane was over Taiwan Island, we believe that the impact of Taiwan Island on the typhoon was not a main factor in the dramatic decrease in the intensity because the main body of the typhoon remained over the sea. Furthermore, sensitivity experiments on the geomorphology of Taiwan Island, in which Taiwan Island was lifted or lowered, obtained the same conclusions. These results will be described in a separate study.

REFERENCES:

- [1] CHEN Lian-shou, DING Yi-hui. Introductory Summary on West Pacific Typhoons [M]. Beijing: Science Press, 1979: 1-491 (in Chinese).
- [2] YAN Jun-yue. Climatological characteristics of rapidly intensifying tropical cyclones over the offshore of China [J]. *J Appl Meteorol Sci*, 1996, 7(1): 28-35 (in Chinese).
- [3] YU Yu-bin, YAO Xiu-ping. A statistical analysis on intensity change of tropical cyclone over Western North Pacific [J]. *J Tropical Meteorol*, 2006, 22(6): 521-526 (in Chinese).
- [4] DUAN Yi-hong, YU Hui, WU Rong-sheng. Review of the research in the intensity change of tropical cyclone [J]. *Acta Meteorol Sinica*, 2005, 63(5): 636-645 (in Chinese).
- [5] YU Yu-bin, CHEN Lian-shou, YANG Chang-xian. The features and mechanism analysis on rapid intensity change of super Typhoon Saomei (2006) over the offshore of China [J]. *Chin J Atmos Sci*, 2008, 32 (2): 405-416 (in Chinese).
- [6] ZENG Zhi-hua, CHEN Lian-shou, WANG Yu-qing, et al. A numerical simulation study of super Typhoon Saomei (2006) intensity and structure changes [J]. *Acta Meteorol Sinica*, 2009, 67(5): 750-763 (in Chinese).
- [7] XU Ying-long, ZHANG Ling, GAO Shuan-zhu. The advances and discussions on china operational typhoon forecasting [J]. *Meteorol Mon*, 2010, 36 (7): 43-49 (in Chinese).
- [8] CHEN Peiyan, YU Hui, CHAN J C L. A Western North Pacific tropical cyclone intensity prediction scheme [J]. *Acta Meteorol Sinica*, 2011, 25(5): 611-624 (in Chinese).
- [9] CHEN Lian-shou, XU Xiang-de, LUO Zhe-xian, et al. An Introduction to Tropical Cyclone Dynamics [M]. Beijing: Meteorological Press, 2002, pp: 1-317.
- [10] EMANUEL K A. Sensitivity of tropical cyclones to surface exchange coefficients and a revised steady-state model incorporating eye dynamics [J]. *J Atmos Sci*, 1995, 52(22): 3 969-3 976.
- [11] EMANUEL K A. A statistical analysis of tropical cyclone intensity [J]. *Mon Wea Rev*, 2000, 128(4): 1 139-1 152.
- [12] ZHANG D L, CHANH Q K. Shear-forced vertical circulations in tropical cyclones [J]. *Geophys Res Lett*, 2005, 32(13): 301-320.
- [13] DeMARIA M. The effect of vertical shear on tropical cyclone intensity change [J]. *J Atmos Sci*, 1996, 53(14): 2 076-2 087.
- [14] YUAN Jia-shuang, ZHENG Qing-lin. Numerical Study of the effect of persistent warmer sea surface temperature in tropical indian ocean on atmospheric circulation in the early summer in East Asia in 1991 [J]. *J Trop Meteorol*, 2004, 10(2): 113-122.
- [15] BAIK J J, PAK J S. A climatology of sea surface temperature and the maximum intensity of Western North Pacific tropical cyclones [J]. *J Meteorol Soc Japan*, 1998, 76(1): 129-137.
- [16] ANDREAS E L, EMANUEL K A. Effects of sea spray on tropical cyclone intensity [J]. *J Atmos Sci*, 2001, 58 (24): 3 741-3 751.
- [17] ZENG Zhi-hua, CHEN Lian-shou, WANG Yu-qing. An observational study of environmental dynamical control of tropical cyclone intensity in the North Atlantic [J]. *Mon Wea Rev*, 2008, 136: 3 307-3 322.
- [18] YU Yu-bin, YANG Chang-xian, YAO Xiu-ping. The vertical structure characteristics analysis on abrupt intensity change of tropical cyclone over the offshore of China [J]. *Chin J Atmos Sci*, 2007, 31 (5): 876-886 (in Chinese).
- [19] HANLEY D, MOLINARI J, KEYSER D. A composite study of the interaction between tropical cyclones and upper-tropospheric troughs [J]. *Mon Wea Rev*, 2001, 129 (10): 2 570-2 584.
- [20] LEI Xiao-tu, TANG Jie, XU Xiao-lin, et al. Dynamic factors related to decay process of offshore tropical cyclones in northwest Pacific [J]. *J Trop Meteorol*, 2012, 18(2): 127-134.

Citation: QIAN Yan-zhen, ZHANG Sheng-jun and CHEN Lian-shou. A study on the mechanism of rapid weakening of typhoon Xangsane (0020) over the East China Sea [J]. *J Trop Meteorol*, 2016, 22(3): 352-361.